Journal of Alloys and Compounds 501 (2010) 42–46

Contents lists available at ScienceDirect

Journal of Alloys and Compounds

journal homepage: www.elsevier.com/locate/jallcom

Strong luminescence of novel water-soluble lanthanide complexes sensitized by pyridine-2,4,6-tricarboxylic acid

Yuan-Yuan Ren [a], Bao-Li An [a,*], Qian Xu [b]

[a] Department of Chemistry, College of Science, Shanghai University, Shanghai, 200444, China
[b] School of Pharmacy, Fudan University, Shanghai, 201203, China

ARTICLE INFO

Article history:
Received 15 January 2010
Received in revised form 24 March 2010
Accepted 1 April 2010
Available online 10 April 2010

Keywords:
Optical materials
Chemical synthesis
Crystal structure
Luminescence

ABSTRACT

Sensitive biological analysis requires optical labels have good water solubility and excellent luminescent properties. Herein, two water-soluble lanthanide (Ln) complexes, $Na_6[Ln(PTA)_3]$ (Ln = Eu and Tb), have been synthesized with a new tridentate ligand, pyridine-2,4,6-tricarboxylic acid (H_3PTA). The two-lanthanide complexes showed great characteristic emissions of Eu^{3+} and Tb^{3+} ions with high quantum yields of 54.3 ± 0.5% and 20.2 ± 0.2%, respectively. Moreover, they have good water solubility and can be labelled on biological molecules by dehydration reactions between the non-coordinated –COOH groups from the luminescent complexes and the $–NH_2$ groups from the biological molecules.

1. Introduction

Since a bright photoluminescence europium complex was firstly reported by Weissman in 1942 [1], stable complexes of luminescent trivalent lanthanide (Ln) ions have received much attention. Lanthanide chelates, especially Sm^{3+}, Eu^{3+}, Tb^{3+} and Dy^{3+} complexes, have drawn considerable interest because of their unique luminescent properties, such as sharp emission lines and long lifetime of the excited states, which provide advantages in time-resolved luminescence detection [2,3]. Furthermore, lanthanide complexes do not suffer much from photobleaching problems while organic dyes do because Ln^{3+} ions are efficient quenchers for the triplet states of most biomolecules. On the other side, lanthanide chelates have smaller physical size than that of quantum dots. In addition, the small Stokes shift of emitting quantum dots makes self-quenching as a serious issue while the fluorescent labels are in high concentrations [4,5]. In recent years, as time-resolved fluorometric analysis technology has developed rapidly, new fluorescence reagents are expected to promote the application of highly sensitive detection technology in biological analysis [6]. Sensitive biological analysis requires optical labels to be water soluble, thermodynamically stable and non-toxic, in addition to possessing adequate luminescent properties [7].

Here, two water-soluble lanthanide complexes (Ln = Eu and Tb) with an organic ligand, pyridine-2,4,6-tricarboxylic acid (H_3PTA), have been synthesized. Interestingly, the single ligand efficiently sensitized europium (III) emission as well as terbium (III) emission (Fig. 1). The crystal structure and luminescence properties of these complexes, $Na_6[Ln(PTA)_3]$ (Ln = Eu and Tb), have also been investigated. Bovine serum albumin (BSA) is one of the most abundant proteins. It has a remarkable ability of binding and transporting materials across cell membrane that makes it ideal for drug delivery and very useful for pharmaceutical industry [8]. BSA was labelled with $Eu(PTA)_3{}^{6-}$ and $Tb(PTA)_3{}^{6-}$, respectively, and the luminescent properties of the labelled BSA were discussed. The good solubility of these complexes in water and their excellent luminescence properties might make them to be attractive luminescent labels of biological molecules.

2. Experimental

2.1. Synthesis

Pyridine-2,4,6-tricarboxylic acid (H_3PTA) was synthesized following a literature method [9] by oxidation of 2,4,6-trimethylpyridine in an aqueous solution of $KMnO_4$ with yield of 50%. IR (KBr): $\nu = 3501.8$ (m, ν(COO-H)), 3157.7 (m, ν(C—H)), 1729.6 (s, ν(C=O)), 1701.7 (s, ν(C=O)), 1614.9 (w, ν(C=N, in Py)), 1568.6 (w, ν(C=C, in Py)). ^1H NMR (400 MHz, DMSO-d_6, δ): 8.52 (s, 2H, in Py).

$Na_6[Ln(PTA)_3]$ (Ln = Eu and Tb) was prepared by adding an aqueous solution of 0.4 mmol $LnCl_3$ (Ln = Eu or Tb) to 1.2 mmol H_3PTA dissolved in water. The pH value of the mixture was adjusted to 8 by adding an aqueous solution of sodium hydroxide, then the mixture solution was stirred for 12 h at 60 °C. White rhombohedral crystals precipitated from the solution after deposited for 96 h at room temperature. The crystals were hydrated complexes, $Na_6[Ln(PTA)_3]$ (Ln = Eu and Tb), with yields of 53% and 56%, respectively. The elemental analysis results for $Na_6[Eu(PTA)_3]\cdot 16.5H_2O$ are: found (calcd for $Na_6EuC_{24}H_{39}N_3O_{34.5}$) C 23.22 (23.79), H 3.28 (3.24), N 3.41 (3.47). IR (KBr): $\nu = 3427.1$ (s, ν(COO–H)), 1618.3 (s, ν(C=O)), 1556.4 (m, ν(C=N, in Py)), 1439.9

---

[*] Corresponding author. Tel.: +86 21 66132670; fax: +86 21 66134594.
E-mail address: blan@staff.shu.edu.cn (B.-L. An).

0925-8388/$ – see front matter © 2010 Elsevier B.V. All rights reserved.
doi:10.1016/j.jallcom.2010.04.025

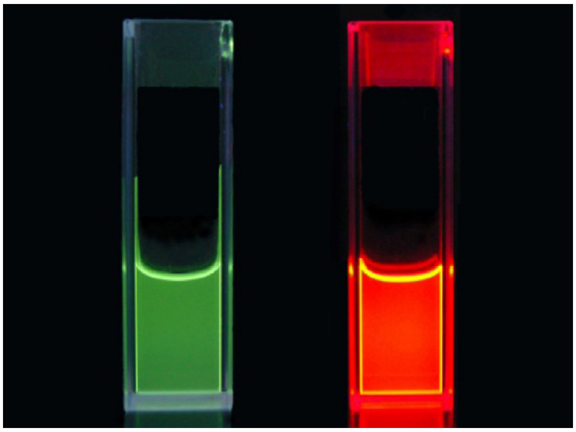

Fig. 1. Photograph of 0.05 mol L^{-1} $Ln(PTA)_3{}^{6-}$ complexes in water solutions under excitation by a standard laboratory UV lamp (λ_{ex} = 254 nm), Ln = Tb and Eu from left to right.

(m, ν(C=C, in Py)), 1365.8 (s, ν(C=O)), 467.4 (w, ν(Eu–O)). The elemental analysis results for $Na_6[Tb(PTA)_3]\cdot 16.5H_2O$ are: found (calcd for $Na_6TbC_{24}H_{39}N_3O_{34.5}$) C 23.12 (23.66), H 3.28 (3.23), N 3.38 (3.45). IR (KBr): ν = 3441.5 (s, ν(COO–H)), 1625.6 (s, ν(C=O)), 1557.2 (m, ν(C=N, in Py)), 1436.6 (m, ν(C=C, in Py)), 1366.8 (s, ν(C=O)), 455.7 (w, ν(Tb–O)), 405.3 (w, ν(Tb-O)).

2.2. *Crystal structure determination*

Diffraction intensities for the complex were collected at 20 °C on a Siemens R3m diffractometer with the v-scan technique. Lorentz-polarization and absorption corrections were applied [10]. The structures were solved with the direct method and refined with full-matrix least-squares using the SHELXS-97 and SHELXL-97 programs respectively [11,12]. Anisotropic displacement parameters were applied to all non-hydrogen atoms, and the organic hydrogen atoms were generated geometrically (C–H 0.96 Å), the aqua hydrogen atoms were located from difference maps and refined with isotropic displacement factors. Analytical expressions of neutral-atom scattering factors were employed, and anomalous dispersion corrections were incorporated [13]. Both the crystal data and the data details [14] were collected and refined for the complex, and drawings were produced with SHELXTL [15].

2.3. *Labeling of BSA with $Eu(PTA)_3{}^{6-}$ and $Tb(PTA)_3{}^{6-}$*

$Na_6Eu(PTA)_3$, $Na_6Tb(PTA)_3$ and *N*-hydroxysuccinimide (NHS) were dried in vacuum for 24 h in a desiccator in the presence of P_2O_5. Then, 0.7 mg of NHS and 1 mg of 1-ethyl-3-(3-dimethylaminopropyl) carbodiimide hydrochloride (EDC) were added to the solution of 5 mg of $Na_6Eu(PTA)_3$ in 800 μL of ethanol and 200 μL water, and the solution was shaked for 24 h at 37 °C in the dark. The ethanol was removed by vacuum evaporation. The product was directly used for BSA labelling without further purification. Since $Ln(PTA)_3{}^{6-}$ (Ln = Eu or Tb) and NHS are equimolar, and the three non-coordinated carboxyl groups from $Ln(PTA)_3{}^{6-}$ (Ln = Eu or Tb) have equal chemical activity, it was proposed that only one carboxyl group of the lanthanide complex is esterified in the intermediate compound, NHS-$Ln(PTA)_3$ (Ln = Eu or Tb). NHS-$Ln(PTA)_3$ (Ln = Eu or Tb) was added to 1 mg BSA in 100 μL 50 mmol L^{-1} carbonate buffer of pH 9.6. After shaking for 4 h at 37 °C in the dark, the solution was dialyzed three times against 4 L of 0.01 mol L^{-1} PBS buffer at 4 °C for 48 h.

2.4. *Physical measurements*

Elemental analysis for the samples was carried out with an Elementar vario EL elemental analyzer. UV absorption spectra were recorded on Hitachi U-2900 UV–vis recording spectrophotometer in the region of 200–400 nm. IR spectra in the region of 4000–400 cm^{-1} were recorded on a Bruker infrared spectrophotometer by conventional KBr method. The ^1H NMR spectra were recorded on a USA Varian UNITYINOVA-500 spectrometer (500 MHz). The excitation and emission spectra for the complexes were measured on a Shimadzu RF-5301PC spectrofluophotometer at room temperature. The emission spectra of BSA labelled the complexes were recorded on a Hitachi F-7000 spectrofluophotometer at room temperature.

3. Results and discussion

3.1. *Crystal structure*

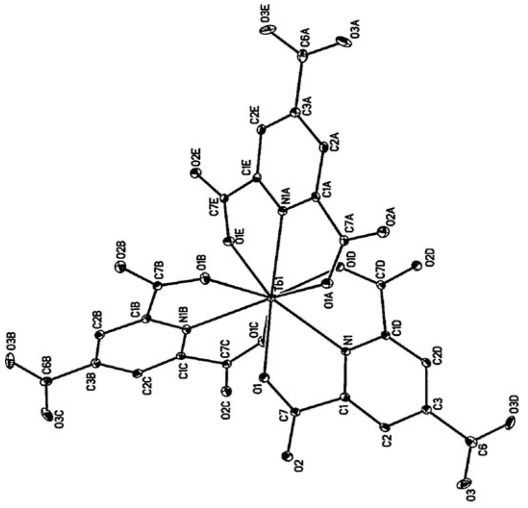

Fig. 2. Crystal structure of $Na_6[Tb(PTA)_3]\cdot 16.5H_2O$.

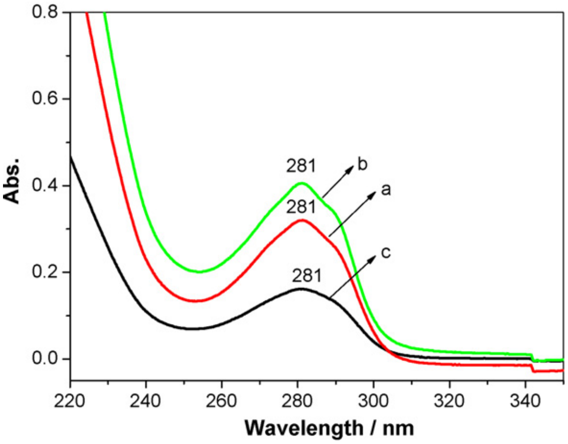

Fig. 3. UV absorption spectra for (a) $Eu(PTA)_3{}^{6-}$, (b) $Tb(PTA)_3{}^{6-}$ and (c) H_3PTA in aqueous solutions (5.0×10^{-5} mol L^{-1}).

The crystal structure of $Na_6[Ln(PTA)_3]\cdot 16.5H_2O$ consists of mononuclear $Na_6[Ln(PTA)_3]$ molecules and lattice water molecules. As shown in Fig. 2, The Tb^{3+} atom coordinated in a tri-capped trigonal prism geometry with three nitrogen atoms [Tb (1)–N (1) 2.531 (7) Å] in pyridine rings and six carboxylate oxygen atoms [Tb (1)–O (1) 2.425 (4) Å] from three different PTA^{3-} ligands. The coordination number of the central Tb^{3+} atom is 9, reaching its coordination-saturated state. Therefore, the lattice water molecules only form donor hydrogen bonds with the carboxylate oxygen atoms. Every lanthanide ion is wrapped thoroughly by three PTA^{3-} ligands, and this kind of structure may be beneficial to good luminescence properties and long lifetime.

3.2. *UV absorption spectra*

UV absorption spectra for dilute H_3PTA and $Ln(PTA)_3{}^{6-}$ (Ln = Eu and Tb) aqueous solutions were determined at the same conditions, the maximum absorption wavelengths and molecular absorption coefficients are given in Table 1. The absorptions for $Ln(PTA)_3{}^{6-}$ (Ln = Eu and Tb) dilute solutions are stronger than that of H_3PTA ligand (Fig. 3), which is attributed to the metal coordination effect. The absorption spectra for $Ln(PTA)_3{}^{6-}$ (Ln = Eu and Tb) aqueous solutions mainly consist of one strong absorption band at 281 nm, which is due to $\pi \rightarrow \pi^*$ absorption from the PTA^{3-} ligand. The lanthanide complexes and the organic ligand showed the same maximum absorption wavelength at 281 nm, which was attributed to that the coordination oxygen atoms from the ligands have no *p*

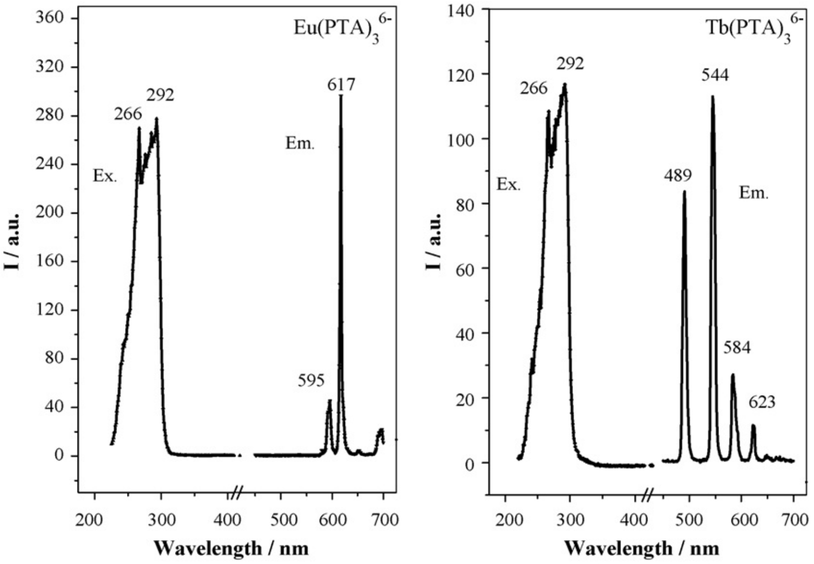

Fig. 4. Excitation and emission spectra for 1.0×10^{-4} mol L^{-1} $Eu(PTA)_3^{6-}$ and $Tb(PTA)_3^{6-}$ in aqueous solutions at room temperature.

electrons to form conjugated rings. In addition, the solubility data for $Na_6Eu(PTA)_3$ and $Na_6Tb(PTA)_3$ in 100 g water are 5.92 g and 5.32 g respectively at room temperature, so, the concentration of the complexes is high enough as luminescent labels of biomolecules in aqueous solutions.

3.3. Luminescence properties

3.3.1. Luminescence properties of the lanthanide complexes

The excitation and emission spectra of $Na_6[Ln(PTA)_3]$ in solid state were determined at ambient temperature. Interestingly, both of the two lanthanide complexes show their characteristic narrow peak emissions. Very bright red characteristic emission of Eu^{3+} from $Na_6[Eu(PTA)_3]$ was observed under violet light excitation (Fig. 4), and the emission peaks were due to f–f electron transition of Eu^{3+} ions from $^5D_0$ to ^7F_J (J = 1 (596 nm), 2 (618 nm), 3 (651 nm), 4 (691 nm)). $Na_6[Tb(PTA)_3]$ showed very bright green characteristic emission of Tb^{3+}, and the four peaks at 493, 543, 583, and 623 nm were assigned to the transition of electrons of Tb^{3+} ions from $^5D_4$ to ^7F_J (J = 6, 5, 4, 3).

The calibration curves for $Eu(PTA)_3^{6-}$ and $Tb(PTA)_3^{6-}$ in 0.01 mol L^{-1} PBS buffer (pH 7.4) are shown in Fig. 5. The detection limits of $Eu(PTA)_3^{6-}$ and $Tb(PTA)_3^{6-}$ were calculated respectively as the concentration corresponding to two standard deviations (SD) of the background intensity, and they were 8.13×10^{-6} and 8.27×10^{-6} mol L^{-1} for the europium and terbium complexes, respectively.

3.3.2. Luminescence properties of BSA labelled $Ln(PTA)_3^{6-}$ (Ln = Eu or Tb)

BSA was successfully labelled with $Eu(PTA)_3^{6-}$ and $Tb(PTA)_3^{6-}$, respectively by synthesizing the active intermediate complex, NHS-$Ln(PTA)_3$ (Ln = Eu or Tb). The labelling scheme is given in Fig. 6.

The emission spectra for BSA labelled with $Eu(PTA)_3^{6-}$ (or $Tb(PTA)_3^{6-}$) and free BSA were determined at the same conditions, and the spectra for the samples were recorded under excitation at 280 nm. As shown in Fig. 7, both BSA-$Eu(PTA)_3$ and BSA-$Tb(PTA)_3$ display their characteristic emission of Eu^{3+} and Tb^{3+} ions respectively. Since the lanthanide complexes have long lifetime, so the concentration of BSA may be detected by time-resolved luminescence method.

3.4. Lifetime and quantum yield

Lifetime for the solid europium complex was measured by monitoring the decay curve of emission of Eu^{3+} ions at 618 nm under a pulse excitation at 299 nm, and the lifetime for the solid terbium complex was obtained by monitoring the decay curve of emission at 543 nm under a pulse excitation at 341 nm (Fig. 8). Both the europium complex and the terbium complex in solid state have very long lifetimes of 1.368 ± 0.001 and 1.441 ± 0.001 ms, respectively. Lifetimes for these complexes in dilute aqueous solutions (0.05 mol L^{-1}) were also obtained by the above-mentioned ways under a pulse excitation at 280 nm. The lifetimes for $Eu(PTA)_3^{6-}$ and $Tb(PTA)_3^{6-}$ in dilute water solutions are 1.470 ± 0.001 and 0.506 ± 0.001 ms, respectively. The results indicate that these complexes have long enough luminescence lifetimes for applications in time-resolved luminescence analysis.

The luminescence quantum yields for $Na_6[Ln(PTA)_3]$ (Ln = Eu and Tb) complexes in dilute aqueous solutions were measured by comparison with two luminescence standards [17,18] using the

Table 1
The photophysical properties of H_3PTA and the lanthanide complexes.

Sample	UV absorption		Luminescence		
	λ_{max} (nm)	ε (mol^{-1} dm^3 cm^{-1})	λ_{ex} (nm)	λ_{em} (nm)	I (a.u.)
5×10^{-5} mol L^{-1} H_3PTA	281	3.3×10^3			
5×10^{-5} mol L^{-1} $Eu(PTA)_3^{6-}$	281	9.5×10^3	280	618	296
5×10^{-5} mol L^{-1} $Tb(PTA)_3^{6-}$	281	7.8×10^3	280	545	38.8
5×10^{-5} mol L^{-1} $Eu(DPA)_3^{3-}$ [16]	278	9.8×10^3	280	617	523
5×10^{-5} mol L^{-1} $Tb(DPA)_3^{3-}$ [16]	278	9.9×10^3	280	545	101

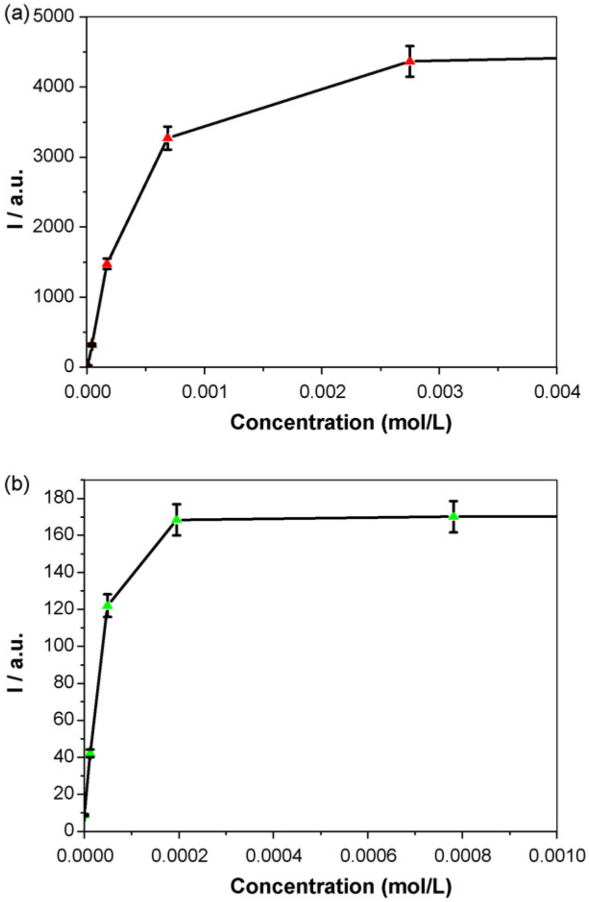

Fig. 5. Calibration curves for (a) $Eu(PTA)_3{}^{6-}$ and (b) $Tb(PTA)_3{}^{6-}$ in 0.01 mol L^{-1} PBS buffer, pH 7.4.

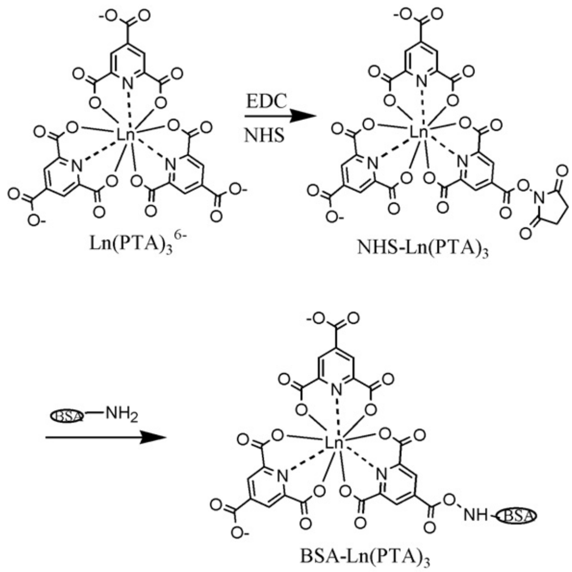

Fig. 6. The labelling scheme for BSA-$Ln(PTA)_3{}^{6-}$ (Ln = Eu and Tb).

Table 2
Quantum yield data of $Na_6[Ln(PTA)_3]$ (Ln = Eu and Tb).

Sample	*A*	$\Delta\Phi$	*q* (%)
5.70×10^{-5} mol L^{-1} $Na_3[Eu(DPA)_3]$	0.477	4280	81.1
5.70×10^{-5} mol L^{-1} $Na_6[Eu(PTA)_3]$	0.541	3255	54.3 ± 0.5
5.65×10^{-5} mol L^{-1} $Na_3[Tb(DPA)_3]$	0.467	16462	86.4
5.65×10^{-5} mol L^{-1} $Na_6[Tb(PTA)_3]$	0.445	3669	20.2 ± 0.2

following formula:

$$q_x = \left(\frac{A_s}{A_x}\right)\left(\frac{\Delta\Phi_x}{\Delta\Phi_s}\right) q_s$$

A_s and A_x are the absorbance of the standard and the sample at 280 nm, respectively, and q_s and q_x are the quantum yields for the standard and the sample respectively. The terms of $\Delta\Phi_x$ and $\Delta\Phi_s$ are the integrated photon flux for the sample and the standard respectively. Experimental quantum yields for $Na_6[Ln(PTA)_3]$ (Ln = Eu and Tb) in aqueous solutions (PBS buffer, pH 7.4) at 295 K are given in Table 2. The Eu^{3+} complex in dilute water solution has high quantum yield of 54.3 ± 0.5% under violet light excitation. $Na_6[Tb(PTA)_3]$ exhibits shorter lifetime and lower quantum yield than those of $Na_6[Eu(PTA)_3]$ in aqueous solution. As Fig. 9 shown, the lowest triplet state ($T_1(L)$) of H_3PTA ligand matches the $^5D_0$ excited state of Eu^{3+} ions better than the $^5D_4$ excited state of Tb^{3+} ions according to the energy gap study on the Eu^{3+} and Tb^{3+} β-diketonate chelates [19]. So, the europium complex showed

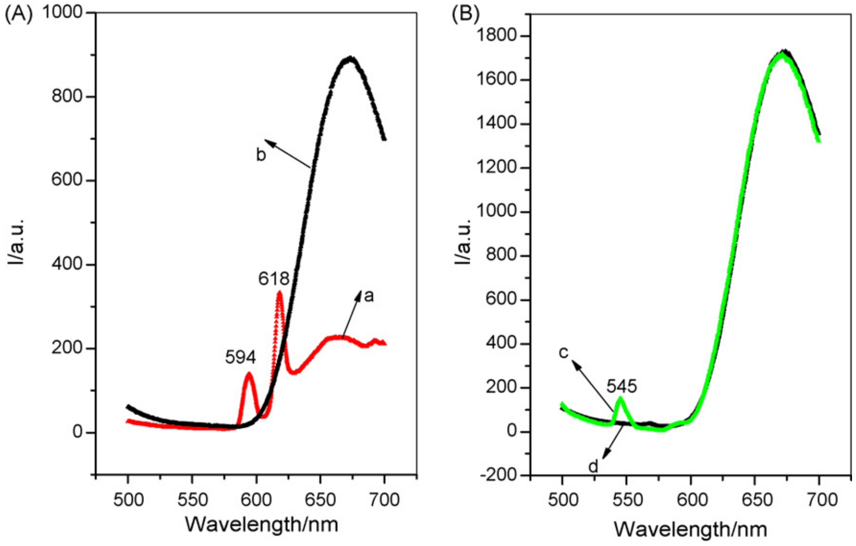

Fig. 7. Emission spectra for (a) BSA-$Eu(PTA)_3$, (b) free BSA, (c) BSA-$Tb(PTA)_3$ and (d) free BSA in 0.01 mol L^{-1} PBS buffer.

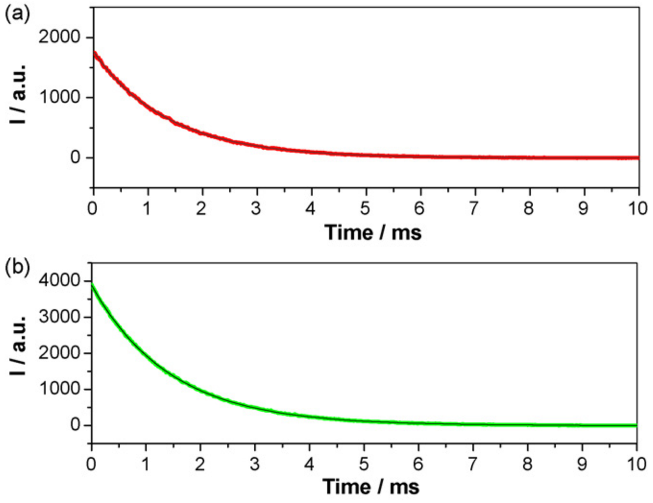

Fig. 8. Lifetime decay curves for (a) $Na_6[Eu(PTA)_3]$ and (b) $Na_6[Tb(PTA)_3]$ in solid state.

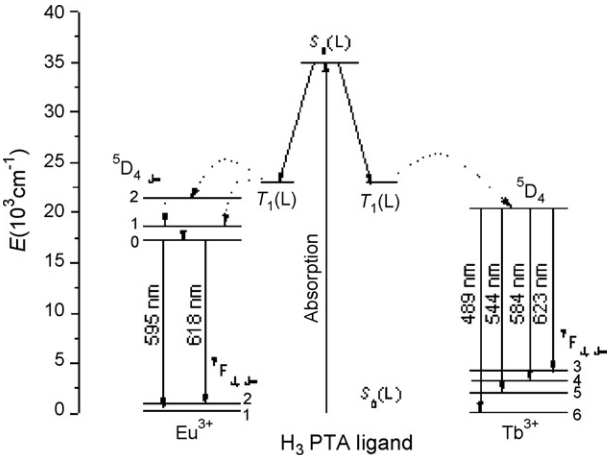

Fig. 9. Energy transfer scheme.

higher quantum yields either in solid state or in aqueous solution. But the energy gap between the $T_1(L)$ and the $^5D_4$ state of Tb^{3+} ions was proposed to be a little narrow, hence the energy was partially lost in the electron transfer process from $T_1(L)$ to $^5D_4$ in aqueous solution. So, $Na_6[Tb(PTA)_3]$ exhibits shorter lifetime and lower quantum yield than those of $Na_6[Eu(PTA)_3]$ in aqueous solution.

4. Conclusions

Characteristic luminescence of Eu^{3+} and Tb^{3+} can be efficiently sensitized by a same organic tridentate ligand, pyridine-2,4,6-tricarboxylic acid. Each Eu^{3+} and each Tb^{3+} ions are wrapped perfectly by three PTA^{3-} ligands, and no water or solvent molecule coordinate to the lanthanide ions directly in solid state. Additionally, the complexes show very strong luminescence in the visible region under violet excitation light. BSA can be labelled with $Eu(PTA)_3{}^{6-}$ and $Tb(PTA)_3{}^{6-}$ under gentle reaction conditions by dehydration reactions of the –COOH groups from the lanthanide complexes and the $-NH_2$ groups from the BSA. The good solubility of these complexes in water and their excellent luminescent properties may make them to be attractive candidates as luminescent label probes in biological systems.

Acknowledgements

This work was supported by the fund of Shanghai Municipal Education Committee (2006AZ071), and Fund of Fifth Key Discipline of Shanghai Education Committee (No. J50102).

References

[1] S.I. Weissman, J. Chem. Phys. 10 (1942) 214.
[2] J.-C.G. Bünzli, C. Piguet, Chem. Soc. Rev. 34 (2005) 1048.
[3] J.-C.G. Bünzli, Acc. Chem. Res. 39 (2006) 53.
[4] X. Michalet, F.F. Pinaud, L.A. Bentolila, J.M. Tsay, S. Doose, J.J. Li, G. Sundaresan, A.M. Wu, S.S. Gambhir, S. Weiss, Science 307 (2005) 538.
[5] J.P. Zimmer, S.-W. Kim, S. Ohnishi, E. Tanaka, J.V. Frangioni, M.G. Bawendi, J. Am. Chem. Soc. 128 (2006) 2526.
[6] Zhiqiang Ye, Mingqian Tan, Guilan Wang, Jingli Yuan, Anal. Chem. 76 (2004) 513.
[7] Anne-Laure Gassner, Céline Duhot, Inorg. Chem. 47 (2008) 7802.
[8] Abdelghani Housni, Marya Ahmed, Shiyong Liu, Ravin Narain, J. Phys. Chem. C 112 (2008) 12282.
[9] L. Syper, K. Kloc, J. Mlochowski, Tetrahedron 36 (1980) 123.
[10] A.C.T. North, D.C. Phillips, F.S. Mathews, Acta Crystallogr. Sect. A24 (1968) 351–359.
[11] G.M. Sheldrick, SHELXS-97, Program for Crystal Structure Solution, Göttingen University, Germany, 1997.
[12] G.M. Sheldrick, SHELXS-97, Program for Crystal Structure refinement, Göttingen University, Germany, 1997.
[13] D.T. Cromer, International Table for X-ray Crystallography, vol. C, Kluwer Academic Publisher, Dordrecht, 1992 (Tables 4.2.6.8 and 6.1.1.4).
[14] CCDC 748825 contains the supplementary crystallographic data for this paper. These data can be obtained free of charge from The Cambridge Crystallographic Data Centre via www.ccdc.cam.ac.uk/data_request/cif.
[15] G.M. Sheldrick, SHELXTL Version 5, Siemens Industrial Automation Inc., Madison, WI, USA, 1995.
[16] Michael R. George, Christopher A. Golden, Martin C. Grossel, Richard J. Curry, Inorg. Chem. 45 (2006) 1739.
[17] Annina Aebischer, Frédéric Gumy, Jean-Claude G. Bünzli, Phys. Chem. Chem. Phys. 11 (2009) 1346.
[18] Anne-Sophie Chauvin, Frédéric Gumy, Daniel Imbert, Jean-Claude G. Bünzli, Spectrosc. Lett. 37 (2004) 517.
[19] Y.S. Yang, M.L. Gong, Y.Y. Li, H.Y. Lei, S.L. Wu, J. Alloys Compd. 207/208 (1994) 112.